PROCEEDINGS OF SCIENCE

Connection between very high energy events and parsec-scale jet behavior in the TeV quasar 1222+216

Svetlana Jorstad*
IAR, Boston Univ., 725 Commonwealth Ave., Boston, MA 02215, USA
St.-Petersburg State University, 198504 St.-Petersburg, Russia
E-mail: jorstad@bu.edu

Alan Marscher
IAR, Boston Univ., 725 Commonwealth Ave., Boston, MA 02215, USA
E-mail: marscher@bu.edu

Ivan Troitskiy
St.-Petersburg State University, 198504 St.-Petersburg, Russia
E-mail: troitsky@gmail.com

Valeri Larionov
St.-Petersburg State University, 198504 St.-Petersburg, Russia
E-mail: vlar@astro.spbu.ru

Daria Morozova
St.-Petersburg State University, 198504 St.-Petersburg, Russia
E-mail: comitcont@gmail.com

Mark Gurwell
Harvard-Smithsonian Center for Astrophysics, Cambridge, MA, USA USA
E-mail: mgurwell@cfa.harvard.edu

The Boston University blazar research group has been monitoring a sample of γ-ray blazars with the Very Long Baseline Array at 43 GHz since the launch of the *Fermi* Gamma-ray Space Telescope. The sample includes three gamma-ray quasars, 1222+216, 3C279, and PKS1510−089, which have been recently detected at E>0.1 TeV (VHE) with Cherenkov telescopes. The quasar 1222+216 has flared already twice at VHE γ-rays during the *Fermi* era. We present an analysis of the kinematics of the inner parsec-scale jet of 1222+216 during quiescent states and VHE events and discuss the possible mechanisms for VHE photon production and the location of the VHE emission sites.

4th Annual Conference on High Energy Astrophysics in Southern Africa
25-27 August, 2016
Cape Town, South Africa

*Speaker.

PoS(HEASA 2016)017

1. Introduction

The Boston University blazar group has been performing multi-wavelength (MW) monitoring of a sample of γ-ray blazars since 2007 June. The sample includes 21 flat spectrum radio quasars (FSRQ), 13 objects of BL Lac type (BLLac), and 3 radio galaxy (RG). We carry out monthly imaging of the parsec-scale jets of the sources with the Very Long Baseline Array (VLBA) in total and polarized flux density at 43 GHz (VLBA-BU-Blazar program[1]), and optical photometric and polarimetric observations at the 1.83 m Perkins telescope of Lowell Observatory (Flagstaff, AZ, USA), 40 cm LX-200 Telescope of St. Petersburg State University (St. Petersburg, Russia), and 70 cm AZT-8 Telescope of the Crimean Astrophysical Observatory. We obtain γ-ray light curves of the sources using data provided by the Large Area Telescope (LAT) onboard NASA's *Fermi* Gamma-ray Space Telescope and construct X-ray and UV light curves of the sources based on the data available from the Swift X-ray Telescope (XRT) and UV/Optical Telescope (UVOT). The calibrated VLBA data and images, and γ-ray, X-ray, and optical light curves, along with curves of optical polarization parameters, can be found at our website: www.bu.edu/blazars/VLBAproject.html. We observe the source at 230 GHz(1.3 mm) with the Sub-Millimeter Aray (SMA, Mauna Kea, Hawaii, USA)[8].

Of these 37 γ-ray sources in our sample 11 objects have been detected at very high energies (VHE), E>0.1 TeV, by different Cherenkov telescopes. Although the majority of them are BLLacs, the list of VHE sources includes also three quasars, 1222+216, 3C279, and PKS1510-089, and the radio galaxy 3C 84. It is commonly accepted that BLLacs and FSRQs have different environments close to the black hole (BH). Quasars possess an accretion disk (AD), which can dominate the emission at UV and optical wavelengths, as well as clouds of dense gas, which produce broad emission lines, known as broad line region (BLR). The AD emission in BLLacs appears to be suppressed (e.g., [7, 26]), and optical spectra are featureless (e.g, [6]). In the majority of γ-ray quasars the γ-ray emission dominates the spectral energy distributions (SEDs) by up to 3 orders of magnitude relative to the other wavebands during strong γ-ray outbursts (e.g. [1] and [3]). Such SEDs challenge the standard synchrotron self-Compton (SSC) models for high energy production, while they can be well explained by models involving Comptonization of radiation provided by the BLR (e.g. [24]), or a dusty molecular torus [20], external inverse Compton models (EC). However, for quasars detected at VHE, the radiation field within the BLR is too opaque to allow VHE photons, up to $\sim$400 GeV, to escape the BLR [4]. This questions the idea that γ-ray production in VHE quasars occurs at sub-parsec distances from the BH. Although a dusty molecular torus is located within a few parsecs from the BH (e.g. [16]), there are arguments that it is too small and confined too close to the equatorial plane of the system to play a significant role in providing seed photons for upscattering to high energies [11]. In this paper we discuss the properties of the parsec-scale radio jet of the quasar 1222+216 (4C+21.35) in connection with the VHE emission. We argue in favor of a site for VHE production in the vicinity of the mm-wave VLBI core located $\sim$10 parsecs from the BH.

[1] www.bu.edu/blazars/VLBAproject.html

2. VHE Detections of 1222+216

The quasar 1222+216 (z=0.432) was observed by the Major Atmospheric Gamma Imaging Cherenkov (MAGIC) telescopes from 2010 May 3 to June 19. The observations were triggered by *Fermi* LAT collaboration Atel #2584 issued on 2010 April 26 that reported a daily increase of flux of the quasar (E>100 MeV) by a factor of 4 with respect to the average flux level. On 2010 June 17 MAGIC detected 1222+216 during a short integration time of 0.5 hr [4]. The signal was strong with a statistical significance of 10.2σ. The energy spectrum extended up to 400 GeV with a photon index $\Gamma_{VHE} = 3.75 \pm 0.27$, while the de-absorbed spectrum with the EBL model of [9] has $\Gamma_{int} = 2.72 \pm 0.34$. The *Fermi* LAT observed a strong flare lasting $\sim$3 days and peaking on 2010 June 18 [21]. Tanaka et al. (2011) found that the HE spectrum from 0.1 to 200 GeV during the peak can be fitted very well by a broken power law with $\Gamma_{LE} = 2.00 \pm 0.05$ and $\Gamma_{LE} = 2.44 \pm 0.10$ and the break photon energy $E_{br} = 1.7^{+1.1}_{-0.4}$ GeV. This implies that the observed simultaneous VHE and GeV spectra between 3 GeV and 400 GeV can be described by a single power law with index $\sim$2.7$\pm$0.3. Based on this result [4] have concluded that "the 100 MeV - 400 GeV emission belongs to a unique component, peaking at $\sim$2-3 GeV, produced in a single region of the jet," outside the BLR. Another extreme property of the VHE outburst of 1222+216 on 2010 June 17 was a very short timescale of variability, when the flux at $E >$100 GeV doubled in $\sim$10 min ([4]), implying that this single region of VHE emission should be extremely compact, $R \sim 1.3 \times 10^{14} (\delta/10)$ cm, where δ is the Doppler factor.

A new state of VHE activity of 1222+216 was observed at the beginning of 2014 when a very bright optical outburst was reported by [15], followed by detection of persistent VHE emission of the quasar by the Very Energetic Radiation Imaging Telescope Array System (VERITAS) [14] and measurements of an increase of the γ-ray flux with $E > 100$ MeV by a factor of 2 in 48 hrs by AGILE (Astrorivelatore Gamma ad Immagini ultra LEggero)[25]. The properties of the VHE emission were different during this outburst with respect to the previous one, with a constant flux over the 10 nights of observation (from 2014 February 26 to March 10), with a total exposure of 5.9 hr.

3. Kinematics of the Parsec-Scale Jet of 1222+216

Within our VLBA-BU-Blazar program we have obtained 76 epochs of total and polarized intensity images of the quasar 1222+216 at 43 GHz from 2007 June to 2015 December. The data were reduced and modeled in the same manner as described in [12]. As mentioned by [21] the source was not bright enough during the first three months of the Fermi mission to be included in the Fermi-LAT Bright Source List [2] despite the source having been detected by EGRET[13]. The analysis of the VLBA images indicates that from 2007 to the middle of 2009 the parsec-scale jet of 1222+216 was in a quiscent state, with the flux density of the core at 43 GHz being less than 0.4 Jy. Starting in the second half of 2009, the core flux density began to rise along with the appearance of bright moving knots in the extended jet. The reader can see a movie at our website (http://www.bu.edu/blazars/), which follows the evolution of the jet on milliarcseconds (mas) scales. We have detected 9 moving knots, $B1 - B9$. Their separation from the core, $A0$, as a function of time is shown in Figure 1 *left*, while Figure 1 *middle* gives the trajectories of

knots projected on the plane of the sky. In addition to the core, we also identify a stationary feature, $A1$, which has a proper motion, $\mu = 0.011 \pm 0.08$ mas yr^{-1}, similar to its 1σ uncerainty. Feature $A1$ is fairly bright, with an average flux density of 0.219±0.095 Jy. It is located at a distance of 0.160±0.025 mas from the core, and its position angle with respect to the core, Θ, varies significantly, $\langle\Theta\rangle$=2.4° ± 8.6°. The latter can be connected with different trajectories of superluminal knots as shown in Figure 1 *middle*, where the direction of trajectories changes from +13° for $B9$ to −10° for $B7$. The moving knots have apparent superluminal velocities, β_{app}, ranging from 12 c to 25 c. Five knots, $B2-B6$, have non-ballistic motion and accelerate, most likely, after the passage through feature $A1$. Table 1 gives the kinematics of knots $B1-B9$ with cosmological parameters as follows: H$_\circ$=70 km s^{-1}Mpc^{-1}, Ω_Λ=0.7, Ω_M=0.3.

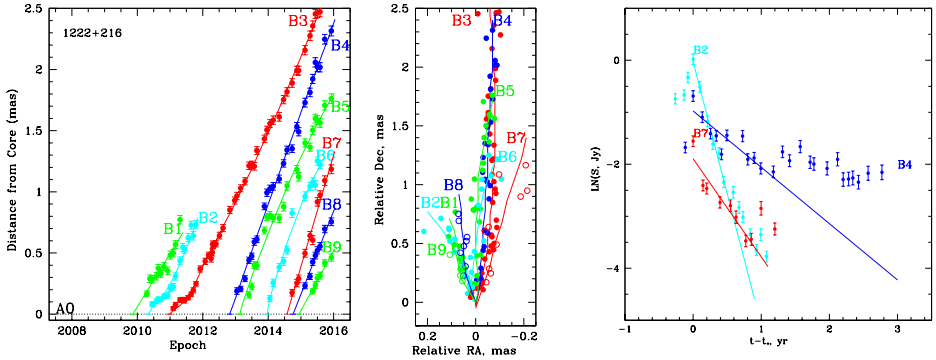

Figure 1: *Left:* Distance of moving knots $B1$(green), $B2$(cyan), $B3$(red), $B4$(blue), $B5$(green), B6(cyan), B7(red), B8(blue), and B9(green) with respect to the presumably stationary core, $A0$, shown by a dotted black line; the solid lines/curves show approximations of the motion by polynomials of order 1-3, which give the best fit to the data according to the χ^2 test. *Middle:* The trajectories of knots $B1-B9$ with respect to the core located at position (0,0). *Right:* Examples of light curves of knots on a logarithmic scale; the solid lines give the rate of fading of the flux density of the knots near the core.

We use the radio light curve of each knot to determine the Doppler factor by applying an approach suggested in [12]: $\delta_{var} = s \times D/[c\, t_{var}(1+z)]$, where D is the luminosity distance, c is the speed of light, s=1.6a is the average size of a knot for a uniform face-on disk that is equivalent to a Gaussian modelfit with FWHM=a, and t_{var} is the variability timescale. However, t_{var} is calculated in a slightly different way than proposed in [12]. We approximate the observed flux density, S, of a knot by an exponential function depending on time as $\ln(S) = k(t-t_\circ) + const$, where $t_\circ$ is the epoch of the global maximum in the light curve and $t_\circ < t < (t_\circ + 1)$, which means that we consider measurements only within 1 yr after the global maximum. Figure 1(*right*) plots several examples of light curves and their approximation in the vicinity of the peak of knot flux density. We calculate coefficients k based on the least squares method and determine timescales of variability as $t_{var} = |1/k|$, which allows us to obtain variabilty Doppler factors. We use δ_{var} and β_{app} of each knot to esimate the Lorentz factor, Γ, and intrinsic viwing angle, $\Theta_\circ$. Table 2 lists derived physical parameters of $B1-B9$.

Analysis of the parameters listed in Table 2 suggests that there is significant variabilty of the physical parameters of disturbances in the jet, with the Lorentz factor changing from 12 to 50, Doppler factor varying from 3 to 20, and viewing angle from 3° to 8°.

Table 1: Kinematics of Superluminal Knots

Knot	N	S, Jy	Θ, deg	μ, mas yr^{-1}	β_{app}, c	$T_\circ$	$T_\circ^*$
B1	12	0.082±0.097	9.3±1.8	0.449±0.022	11.92±0.58	2009.86±0.11	5146±40
B2	16	0.276±0.304	11.3±4.2	0.520±0.016	13.81±0.42	2010.33±0.08	5318±29
B3	44	0.268±0.235	−3.3±6.3	0.495±0.009	13.15±0.23	2010.98±0.09	5555±33
B4	25	0.175±0.089	−2.7±1.2	0.749±0.005	19.88±0.13	2012.82±0.07	6227±26
B5	21	0.116±0.056	−1.1±1.3	0.604±0.006	16.05±0.16	2013.13±0.10	6340±37
B6	12	0.072±0.081	−0.9±3.6	0.706±0.012	18.75±0.33	2013.96±0.09	6642±33
B7	10	0.073±0.053	−9.8±3.9	0.918±0.020	24.38±0.54	2014.57±0.05	6866±18
B8	8	0.218±0.079	6.8±2.9	0.690±0.031	18.32±0.83	2014.70±0.09	6913±33
B9	6	0.253±0.088	13.3±2.8	0.492±0.052	13.06±1.37	2014.94±0.11	7001±40

Notes:
N - number of epochs of knot observations, S - average flux density in Jy and its standard deviation; Θ - average position angle with respect to the core in degree and its standard deviation; μ - proper motion in mas/yr and its 1σ uncertainty, in the case of $B2-B6$ this is the average proper motion; β_{app} - apparent speed in units of the speed of light and its 1σ uncertainty; $T_\circ$ - time of knot ejection in years, which is the time of the passage of centroid of knot through centroid of the core according to extapolation of knot motion back to the core and its 1σ uncertainty; and $T_\circ^*$ - time of knot ejection in RJD, RJD=JD-2450000.0

Table 2: Physical Parameters of Superluminal Knots

Knot	β_{app},c	a, mas	t_{var}, yr	δ_{var}	Γ	$\Theta_\circ$, deg
B1	11.92±0.58	0.10±0.03	0.446±0.090	9.4±2.4	12.3±1.8	5.9±0.9
B2	13.81±0.42	0.09±0.06	0.197±0.012	19.2±3.5	14.6±2.9	2.8±0.6
B3	13.15±0.23	0.09±0.04	1.304±0.183	2.9±0.8	31.5±4.9	8.3±1.3
B4	19.88±0.13	0.23±0.14	2.529±0.380	3.8±1.4	53.8±7.6	5.6±1.1
B5	16.05±0.16	0.21±0.09	2.631±0.602	3.4±1.1	40.3±6.8	6.8±1.2
B6	18.75±0.33	0.17±0.09	0.481±0.245	14.8±3.7	19.3±5.2	3.8±1.0
B7	24.38±0.54	0.19±0.09	0.530±0.131	15.1±3.4	27.3±5.2	3.4±0.7
B8	18.32±0.83	0.13±0.03	0.565±0.091	9.7±1.9	22.3±2.7	4.9±0.6
B9	13.06±1.37	0.11±0.03	0.934±0.715	4.9±2.6	19.8±6.2	7.7±2.4

4. Multi-Frequency Light Curves

Figure 2 *left* shows the γ-ray, X-ray, optical, and mm-wave light curves. Details about the construction of the high energy and optical light curves can be found in [26]. There are two periods of enhanced γ-ray activity: the first one (PI) starts in the middle of 2009 and continues to the end of 2010, the second one (PII) starts in the middle of of 2013 and continues to the end of 2014. Each period has several fast flares with a duration of a couple of weeks when the γ-ray flux exceeds the γ-ray flaring level defined as $\langle F_\gamma\rangle + 3\sigma_\gamma$, where $\langle F_\gamma\rangle$ is the weighted averaged γ-ray flux of 1222+216 and σ_γ is its standard deviation. We have detected 3 and 4 superluminal knots ejected during the first and second periods of γ-ray activity, respectively. There are also two knots, $B4$ and $B5$, ejected during a very modest increase of the γ-ray flux in the end of 2012, with $B4$ and $B5$ having the lowest δ_{var} among the knots. Although the X-ray light curve is fairly sparse, it suggests a modest increase of the X-ray flux during PI and PII. The optical variability appears to correlate with γ-ray variations very well and both mm-wave light curves show similar periods of activity as the γ-ray light curve. In the middle of each period the quasar was detected at E$>$ 100 GeV.

We have determined durations of the periods of γ-ray activity, which have very similar values for PI and PII, 533 and 541 days, respectively, requiring that during an active period F_γ does not fall below $\langle F_\gamma\rangle$ for more than 2 successive measurements. Figure 2 *right* shows the γ-ray light curves

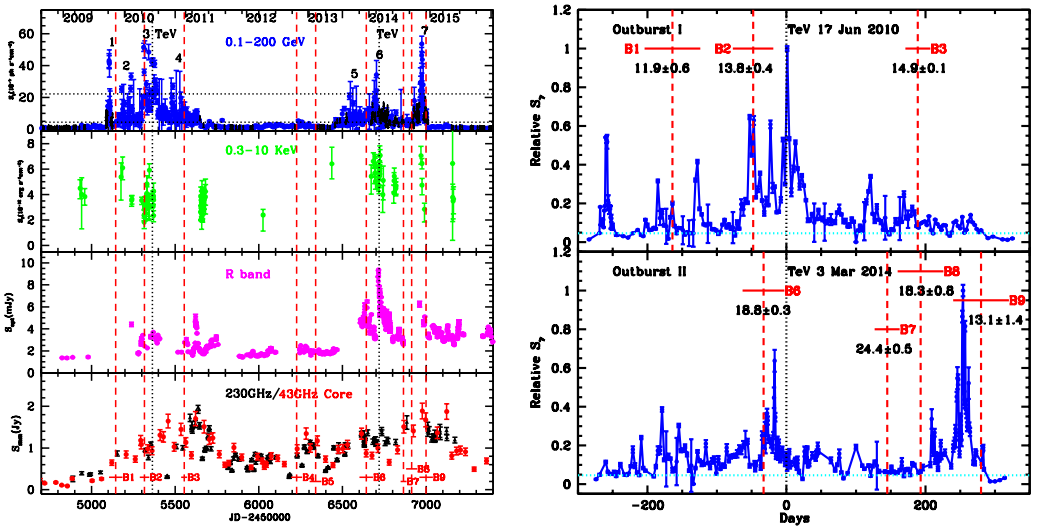

Figure 2: *Left:* MW light curves of 1222+216, from the top: 1. Gamma-ray light curve, horizontal black dotted lines mark the quiescent and flaring levels of γ-ray emission and numbers designate γ-ray flares with flux exceeding the flaring level; 2. X-ray light curve; 3. Optical light curve in R band; 4. Light curves at 230 GHz (black) and of the VLBI core at 43 GHz (red), the vertical red dashed lines show the time of the ejection of superluminal knots, the vertical black dotted lines show the times of peaks of TeV detections. *Right:* The normalized γ-ray light curves during the first (top) and second (bottom) periods of γ-ray activity, with time indicated relative to the peak of the TeV detection during each period (dotted black line), the red vertical dashed lines mark the times of ejection of superluminal knots.

for PI and PII normalized to the maximum of each outburst and constructed in times of $(t - t_{TeV})$, where t_{TeV} is the epoch of the VHE maximum. In both cases, there is a knot ejected from the core several weeks before the TeV peak: $B2$ is ejected 49±29 days before TeV-I and $B6$ is ejected 26±33 days before TeV-II. We associate the TeV events with disturbances in the jet based on (1) the good correlations between both the γ-ray and mm-wave and the γ-ray and optical light curves, (2) the similarity between the linear polarization behavior of the jet and at optical wavelengths [23], and (3) the good agreement between the timing of knot ejections and TeV events. In this case the derived delays and proper motions of $B2$ and $B6$ compute the locations of the TeV outbursts, which are 0.067±0.041 mas and 0.051±0.063 mas downstream of the core, respectively, for TeV-I and TeV-II. Figure 3 shows the VLBA images nearest in time to the TeV events (1 week and 3 days apart for TeV-I and TeV-II, respectively), where positions of the core, $A0$, and the knots are marked. The positions of the knots are extrapolated according to their kinematics, although at these epochs the knots are not resolved yet from $A0$ with modelling by Gaussian components.

As seen in Figure 3, in both cases the knots are located in the most polarized part of the jet, with the degree, p, and position angle, χ, of polarization as follows: p_{B2}=8.2±0.9%, χ_{B2}=12.8±1.9°, and p_{B6}=11.9±1.5%, χ_{B6}=7.7±2.0°. In addition, these knots possess smallest viewing angles with respect to the line of sight and highest Doppler factors among $B1-B9$, with average values over $B2$ and $B6$ parameters equal to $\Theta_\circ \sim$3.3° and $\Gamma \sim \delta_{var} \sim$17. This places the VHE events ∼0.06mas downstream of the core, between features $A0$ and $A1$, which corresponds to 0.34pc projected on the plane of the sky and 5.9pc deprojected. According to the TEMZ model [18] for HE and VHE

production, one of possible sources of seed photons for EC models is the Mach disk formed in the center of a recollimation shock if the jet is symmetric. There is theoretical and observational evidence (e.g, [19, 5]) that the mm VLBI core might be a recollimation shock as well as some stationary features observed in the vicinity of the core [12]. In the TEMZ model scenario [18, 17] the proposed location of the TeV events implies that feature $A1$ is the most likely provider of the seed photons for scattering by relativistic electrons up to VHE, when a superluminal knot approaches $A1$.

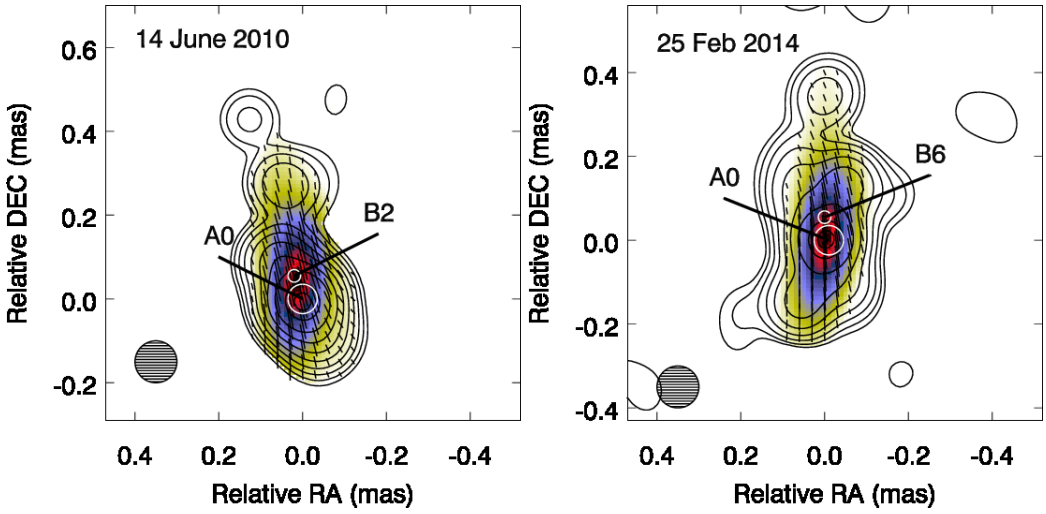

Figure 3: *Left:* The total (contours) and polarized (color scale) intensity image of 1222+216 at 43 GHz on June 14, 2010. *Right:* The total (contours) and polarized (color scale) intensity image of 1222+216 at 43 GHz on February 25, 2014; black line segments indicate direction of linear polarization, and white circles show the size and position of the core and knots $B2$ and $B6$.

5. Conclusion

The quasar 1222+216 is an object that has drawn considerable attention since 2009 when it was first detected in the VHE range. A black hole of $6\times10^8 M_{Sun}$ [10] is located in the center of the quasar, surrounded by an accretion disk with a luminosity of 5×10^{46}erg/s and BLR of size $\sim$0.23pc [22]. A hot dust torus with a luminosity of 2×10^{46}erg/s lies at a distance of $\sim$2pc from the BH [16], and an extremely relativistic jet with $\Gamma \geq 17$ propagates out of the BH at an angle as small as $\sim3^\circ$ to our line of sight.

The 1222+216 system radiates across the electromagnetic spectrum, from 10^9Hz to 10^{26}Hz, exhibits variations at VHE on a timescale as short as 10 min, and contains no break between the HE and VHE spectra [4]. The absence of a spectral cutoff constrains the γ-ray emission region to lie outside the BLR to avoid absorption of VHE γ-rays, while the short timescale of variability restricts the size of the emitting region to $R < 0.014$ pc even with the high Doppler factors that we derive from our VLBA observations. Based on our monitoring of the quasar with the VLBA, contemporaneous with the VHE observations, we place the origin of the VHE events downstream the mm-wave core, when a superluminal knot passes through the "throat" of the jet connecting the mm-wave core and more extended jet, at a distance >6pc from the BH.

Acknowledgement: The research of the BU group presented here was supported by NASA Fermi Guest Investigator grant NNX14AQ58G. The research at St. Petersburg State University was partly funded by RFBR grants 16-32-00036, 15-02-00949 and SPbSU grant 6.38.335.2015.

References

[1] Abdo, A. A., Ackermann, M., Ajello, M, et al. 2011, ApJL, 733, L47

[2] Abdo, A. A., Ackermann, M., Ajello, M, et al. 2009, ApJS, 183, 46

[3] Akyuz, A., Thompson, D. J., Donato, D., et al. 2013, A&A, 556, 71

[4] Aleksić, J., Antonelli, L. A., Antoranz, P, et al. 2011, ApJL, 730, L8

[5] Cawthorne, T. V., Jorstad, S. G., Marscher, A. P. 2013, ApJ, 772, 14

[6] Collinge, M.J., et al. 2005, ApJ, 129, 2542

[7] Giommi, P., et al. 2012, MNRAS, 420, 2899

[8] Gurwell, M. A., et al. 2007, ASPC, 375, 274

[9] Dominguez, A., et al. 2011, MNRAS, 410, 2556

[10] Farina, E. P., et al. 2012, MNRAS, 424, 393

[11] Joshi M., Marscher, A. P., & Boettcher, M. 2014, ApJ, 785, 132

[12] Jorstad, S. G., et al. 2005, AJ, 130, 1415

[13] Hartman, R.C., et al., 1999, ApJS, 123, 79

[14] Holder, J. for the VERITAS collaboration 2014, Atel #5981

[15] Larionov, V. M., et al. 2014, Atel #5921

[16] Malmrose, M., et al. 2011, ApJ, 732, 116

[17] Marscher, A. P. 2016, Galaxy, 4, 37

[18] Marscher, A. P. 2014, ApJ, 2014, 780, 87

[19] Marscher, A. P., et al. 2008, Nature, 2008, 452, 966

[20] Sikora, M. et al. 2009, ApJ, 704, 38

[21] Tanaka, Y. T., et al. 2011, ApJ, 733, 19

[22] Tavecchio, F., et al. 2011, A&A, 534, 86

[23] Troitskiy, I. C., et al. 2016, Galaxy, 4, in press

[24] Vercellone, S., et al. 2011, ApJL, 736, L38

[25] Verrecchia, F., et al. 2014, Atel #6733

[26] Williamson, K. E., et al. 2014, ApJ, 789, 135